Available online at www.sciencedirect.com
SCIENCE DIRECT
Polymer 47 (2006) 5610–5622
polymer
www.elsevier.com/locate/polymer

Ageing of isotactic polypropylene due to morphology evolution, experimental limitations of realtime density measurements with a gradient column

Stefano Piccarolo *

Dipartimento di Ingegneria Chimica dei Processi e dei Materiali, Università di Palermo, Viale delle Scienze, 90128 Palermo, Italy and INSTM Udr Palermo

Received 15 February 2005; accepted 7 March 2005
Available online 12 May 2006

Abstract

Ageing in crystalline polymers is responsible for the deterioration of physical properties leading, for example, to a decrease in toughness and to dimensional changes that are to some extent responsible for warpage and scrap production in injection molding. Since, it depends on the mutual transformation of stable and metastable phases, being always related to changes in morphological organization, it is here preferred to call it 'Morphological ageing'.

Although, one would expect the ageing regime to be determined by the complex morphology with amorphous phases of different mobility and eventually multiple crystalline phases, transformed into each other at an associated transition, existing literature always shows a more trivial linear with the logarithm of time dependence of every probe used to describe ageing.

Existing literature always overlooks the initial morphology, often complex, or, adopts well equilibrated samples, not representative of processing conditions. In this work, ageing of *i*PP was addressed producing samples characterized by an homogeneous morphology even at the largest cooling rates adopted using a CCT approach. This paper describes few of the many attempts undertaken to quantitatively relate ageing to initial morphology in *i*PP melt solidified under conditions emulating polymer processing.

Ageing was monitored by measuring the density time dependence offline, i.e. separately applying the ageing protocol, and online in a gradient column conditioned at the ageing temperature following samples' apparent density evolution. The offline method can give hints about the role of temperature and initial morphology but the results so obtained suffer from significant data scattering. The online method on the other hand, can provide a more accurate interpretation of ageing if due account is made of all the features of the fluid dynamic transient superimposed on the densification due to morphological ageing.

Densification during ageing of the *i*PP samples used, solidified between 1 and 100 °C/s, takes place as a superposition of two phenomena: one is the linear increase of density with the logarithm of time, which is quantitatively related to the initial morphology, i.e. the cooling rate, and the other is a density jump that takes place at times much smaller than the available resolution and thus not quantitatively accessible.

Keywords: Morphological ageing; Density evolution; Post processing

1. Introduction

Although, ageing is usually understood as the change in properties after a long storage time and it is often referred to all kinds of materials, most of the reports on the subject are concerned with ageing in glasses and among them with polymer glass formers, and the phenomenon is called physical ageing [1,2] without implicitly restricting it to polymer glasses. Sometimes mention is made of the behavior of semicrystalline polymers [1,3,4] with an implicit effort to retrace their behavior with that of amorphous glassy polymers. Most of the works concerned with ageing of semicrystalline polymers [5–11] are concerned with time dependent evolution of mechanical properties without a direct link to the morphology responsible for such changes. Since, all the mechanisms occurring involve modifications in morphology we would rather define the changes occurring in semicrystalline polymers upon storage as morphological ageing, as already suggested by Rault [12], thus implicitly referring to the changes in properties resulting from morphological reorganization and hence recognizing the need for addressing the study of morphological changes, or

* Tel.: +39 091 6567225; fax: +39 091 6567280.
E-mail address: piccarolo@unipa.it.

0032-3861/$ - see front matter © 2006 Elsevier Ltd. All rights reserved.
doi:10.1016/j.polymer.2005.03.128

whatever probe related to morphology, to understand ageing in semicrystalline polymers.

The phenomenon we are focusing is well known in the polymer processing community being a severe constraint for production as it can give rise to embrittlement and dimensional instability [13] as well as to warpage [14] thus contributing to scrap production. Often one resorts to time consuming tuning of operating conditions upon changing material batch and even to the modification of processing hardware, i.e. moulds, in an attempt to limit its role. Other applications in which morphological ageing may play a significant role on the decline of physical properties are also known. Nevertheless, the exact mechanisms are often overlooked [15–17] and morphological ageing is confused with the term 'degradation', which is related to chemical changes induced by oxidation, ultraviolet radiation or high temperature intensive melt processing, thus leading to the adoption of useless recipes of chemical stabilizers. However, since the subject is technically relevant particularly in polymer processing, one can find a vast literature on the subject often largely focused on the macroscopic description of typical 'cases' based on particular processing methods and conditions (see [18] and references therein). Obviously, it is not so simple to identify the most relevant mechanisms responsible for warpage and shrinkage in injection molding and it is only recently that the important role of crystallization and its peculiar relevance on this subject has been recognized [19].

Although, this paper is not intended to give a broad review of previous works on the subject, it is nevertheless necessary to cite some of them in order to point out two major limitations usually encountered. The first is related to the approach adopted in schematically ascribing metastability as responsible for the ageing of the amorphous phase only [2], the second refers to the assumption often made in considering bulk samples to be representative of the behavior observed experimentally. The former is due to the misconception of the crystalline phase, in melt solidified polymers, as thermodynamically stable. It has taken long and it has not been easy to realize that polymers, due to their topology, do not give rise to an equilibrium crystalline phase, which will eventually reach an equilibrium thickness only after a long annealing time [12]. One of the limiting steps has been recognized to be the unmixing process between crystallizable and uncrystallizable chain parts, distinguished on the basis of conformationally ordered sufficiently long sequences on one side, and zones where segregation of primary structure defects or of topological constraints is larger on the other [20,21]. Although, the subject has often had the character of an advanced topic [22,23] now the argument has been systematically addressed even on text books [24].

The second limitation can be related to the less prudent assumption often made in considering bulk polymer samples as homogeneous whatever their thermal history was. Although, it is common practice to be cautious with sample thickness especially when deep quenches are adopted, it is not, however, unusual to either not being able to identify the geometrical constraints adopted or find samples of the order of millimeters used for quenches. Alternatively [8], in order to prevent sample not being homogeneous, long annealing procedures are adopted thus supposing the possibility to transfer the ageing behavior observed to real processing conditions where high cooling rates are experienced. One hopefully presumes such information is not used anyway thus neglecting altogether the influence of initial structure on ageing. Even more dramatic is to find out that for such thick samples liquid nitrogen is assumed to be the best cooling medium for applying the largest possible cooling rate thus neglecting the poor thermal exchange coefficient arising due to the onset of the Liedenfrost layer [25] determined by latent heat and temperature of vaporization, both very low for Nitrogen.

2. Model samples from CCT

To bypass these limitations a model experiment, based on the concept of continuous cooling transformation (CCT), borrowed from Metallurgy, has been recently adopted. An empirical approach is used to study structure development at cooling rates comparable to those experienced in most processing techniques, i.e. in the range of 0.1 to above 1000 °C/s. Moreover, it has been possible to obtain significant improvements (as compared to the situation in which CCT is applied to metals) by a careful design of sample holding assembly, geometrical constraints and cooling medium, water being the best for this purpose unless one would consider using a low melting temperature liquid metal, i.e. mercury. The most relevant aspect of this approach lies in the fact that, once some constraints are met [26], the technique allows to obtain large enough samples with an homogeneous morphology. Most of the geometrical limitations are on sample thickness and are inversely related to cooling rate. It is therefore, possible to obtain a sufficiently large sample, which can be used for bulk characterizations of density and wide angle X-ray diffraction (WAXD) dependence on cooling rate as shown in Fig. 1 for an isotactic polypropylene (*i*PP) sample on which this work is mostly centered [27].

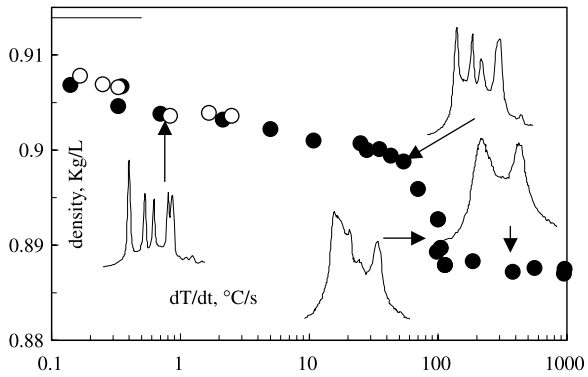

Fig. 1. Solidification curve for *i*PP3 (Table 1) showing the density dependence on cooling rate and some representative WAXD patterns. Filled symbols refer to samples obtained by the CCT procedure while open symbols are obtained by DSC at constant cooling rate. The continuous line on the left ordinate refers to a sample obtained under isothermal conditions at 134 °C until crystallization is complete.

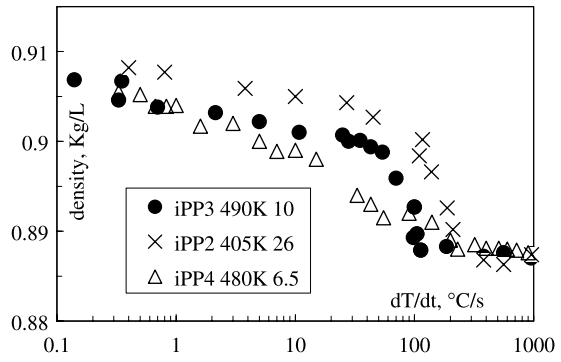

Fig. 2. Influence of molecular weight distribution on the solidification curve of *i*PP, data in the legend refer to M_w and polydispersity also reported in Table 1.

Fig. 1 represents the 'solidification curve', a characteristic feature for the melt solidification of this polymer under quiescent non-isothermal conditions. Both probes shown in Fig. 1, WAXD and density, describe the same changes of structure occurring upon changing cooling rate, although superimposed, they provide different information. At high cooling rates a lower density plateau value is observed for *i*PP where only the so called mesomorphic phase is found. At low cooling rates, a continuous decrease of density with cooling rate is obtained related to the onset of the stable phases whose amount decreases with cooling rate. Often a critical cooling rate, Q_{cr}, is observed where density suddenly falls to the level of the mesomorphic phase. Around Q_{cr} a competition between stable and intrinsically metastable phases takes place often giving rise to a larger uncertainty on density determinations since small modifications of cooling rate give rise to large morphological changes [26].

The solidification curve is not only characteristic of a given polymer class [28], it is also sensitive to changes in molecular weight and nucleating agents, as shown in Figs. 2 and 3, respectively, (Table 1). Fig. 2 shows that a larger polydispersity (M_w/M_n) shifts the Q_{cr} to larger values and makes the range where Q_{cr} occurs sharper, i.e. the density falls from the value of the stable crystalline phase to that of the mesomorphic one in a narrower range of cooling rates. In this context one is clearly inclined to interpret this behavior on the basis of the larger concentration of low molecular weight chains, i.e. of

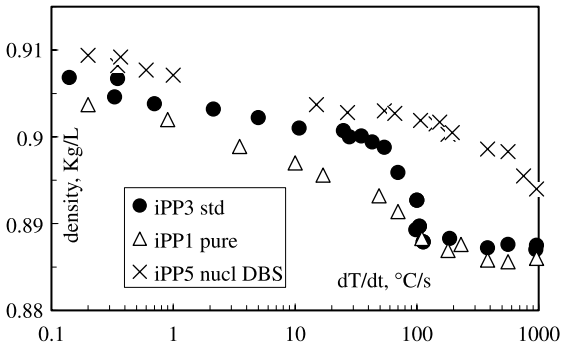

Fig. 3. Influence of nucleating agents on the solidification curve of *i*PP, details of polymer characteristics are shown in Table 1.

Table 1
Characteristics of the isotactic polypropylenes used

Polymer	M_w	M_w/M_n	Nucleant
*i*PP1	476,000	6	
*i*PP2	405,000	26	
*i*PP3	490,000	9,7	
*i*PP4	480,000	6,4	
*i*PP5	483,000	10	DBS 2000 ppm

chain ends, which should play an important role for crystallization at high cooling rates.

Fig. 3 compares three *i*PP grades with quite similar molecular weight but with different contents of nucleating agents. The reference material (*i*PP3) is a standard polymer while *i*PP1 is a so called 'capacitor grade' also known as hyper pure as it is washed of catalyst residues, ash content ca. 15 ppm. Finally, *i*PP5 is similar to *i*PP3 but for the addition of 2000 ppm of a typical polyolefin nucleating agent, DBS. The role of the nucleating agent is evident since the cooling rate range in which the stable α-monoclinic phase can be observed is now extended up to much higher cooling rates as compared to *i*PP3, so high that the plateau density value, characteristic of the mesomorphic phase, is not observed even at the highest cooling rates employed. Fig. 3 also shows that small amounts of catalytic residues are effective nucleating agents as can be noted from the Q_{cr} of *i*PP3, shifted to a higher value than that of the hyper pure *i*PP1.

Also mechanical properties, obtained by conventional uniaxial tensile tests with a draw rate of 5 mm/min at room temperature, show in Fig. 4a similar dependence on cooling rate as density, for the same polymer, *i*PP3, reported in Fig. 1. However, the sharp drop observed at Q_{cr} for density is not observed by the elastic secant modulus nor by the maximum stress, conventionally called as the yield stress. Thus, disappearance of the stable α-monoclinic phases is not accompanied by a parallel drop of mechanical properties. In the Q_{cr} zone the amount of α-monoclinic crystals is very small and sometimes small spherulites can even be observed dispersed in the mesomorphic slightly birefringent medium

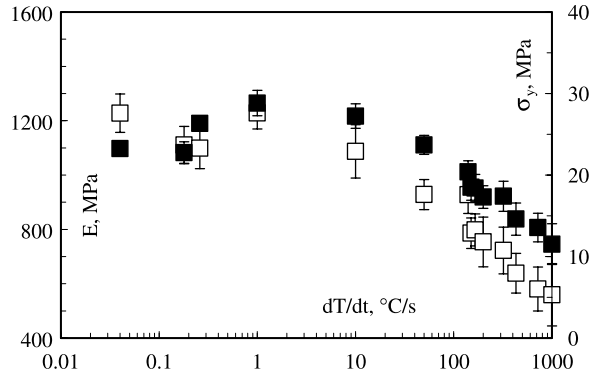

Fig. 4. Influence of cooling rate on the uniaxial tension mechanical properties of films of *i*PP3 solidified by the CCT procedure. Elastic modulus and yield stress are shown as open and filled symbols, respectively, samples size is 20 by 3 mm and thickness is in the range of 0.1–0.2 mm, deformation rate is 5 mm/min.

[27]. The change of mechanical properties is apparently determined by the arrangement of regions with different order rather than by the volumetric amount of the phases, i.e. crystallinity is not sufficient to describe mechanical properties.

3. A brief review of ageing in semicrystalline polymers

Before introducing the method adopted to study ageing in *i*PP and the results obtained it is necessary to briefly summarize previous work. The intention is not to provide an exhaustive overview of ageing in semicrystalline polymers but rather to point out some contradictions between known experimental results and the complex morphology observed.

Ageing of semicrystalline polymers is far more complex than that of amorphous polymers. Struik has already observed different regimes depending on temperature with respect to two glass transitions [3,29], the first, Tβ, being related to the onset of cooperative mobility in the amorphous phase, i.e. the glass transition, and the second, the so called upper glass transition, polymer in a non-crystalline phase arising due to the crystalline phase constraints. Although, this is in line with the occurrence of a rigid amorphous phase (RAP), determining many physical properties of crystalline polymers [30], in the case of *i*PP the nature of the RAP, sometimes identified as mesomorphic [31] or locally conformationally ordered [32], further complicates the interpretation. Furthermore, it is clear that an internal friction at a temperature Tαc causes a peculiar behavior since above this temperature onset of mobility in the crystalline phase [33] takes place. Hence, the name Tαc, where 'α' stands for the highest transition occurring in the solid.

Tαc may often be confused, since largely superimposed, with the upper glass transition [29], or the conceptually similar T*, due to the onset of mobility in the intermediate layer mesomorphic phase [31] indicating that a clear interpretation of the phenomenon is still missing and what determines their absolute values is still under debate [34]. It is, however, clear that T* depends on thermal history and it is lower than Tαc while the latter is closely related to the thickness of the crystalline phase [12,29]. Tαc evolves, for a constant annealing (ageing) temperature, towards an equilibrium value bringing Rault to hypothesize that Tαc is roughly equivalent to the ageing temperature and in turn equivalent to the crystallization temperature in case the material is solidified from the melt isothermally [12]. This scheme, which may be effective to ageing in some cases [35], might not generally apply. For some polymers Tαc can be so close to the melting temperature that it becomes unrealistic to speak of ageing under these conditions [21]. NMR investigations have recently provided a sound interpretation of Tαc for several polymers [35] as the onset of helical jumps in the crystalline phase. The process has been observed to be responsible for room temperature ultradrawability and for ageing in *i*PP where the αc process gives rise to conversion of non-crystalline protons to crystalline ones almost independently of tacticity and molecular weight distribution [36]. Above the threshold determined by Tαc an irreversible process of crystallinity increase takes place, whether it is called secondary crystallization [37], stabilization [38] or annealing [20]. These views, which are only apparently different, might, however, be reconciled under the multi-step concept of polymer crystallization recently advanced by Strobl [38].

Other phenomena more specifically related to the metastability of the crystalline phase formed upon solidification from the melt may also occur. One example is the most evident room temperature phase II to I transition occurring in polybutene1, which again depends on initial morphology [39]. Such transformations all need mobility in the crystalline phase, i.e. temperatures above the crystalline phase Tαc, a priori different for each phase and in dependence of their own crystallite size, the latter playing an important role to determine their relative stability [40].

A further mechanism for crystallinity increase, especially important for low crystallinity and high Tαc polymers, is the one properly called secondary crystallization [41,42] by which new lamellae are inserted between those formed during the primary crystallization. This mechanism occurs since the regions remaining amorphous still have the potential to partially crystallize. Moreover, the intervening lamellae are constrained by those formed during primary crystallization, which are thicker as they are formed at higher temperatures. Because an additional driving force is needed, the intervening lamellae develop at lower temperatures upon further non-isothermal cooling, with smaller thickness obeying the Gibbs–Thomson equation. Since, their Tαc depends on their thickness their stability is also smaller. They may thicken if a low temperature active Tαc process is plausible (*i*PP, PE). Otherwise they may melt and recrystallize upon heating, (PET).

Under this complex scenario it is not easy to recognize different regimes, which might take place depending on the mechanisms activated by the external ageing conditions adopted. It is not only a matter of ageing temperature with respect to the Tβ, T*, Tαc transitions since Tαc and T*, mutually influencing each other, depend on morphology and keep on changing with ageing [12]. Such scenario would even question the possibility to quantitatively describe ageing in crystalline polymers and probably this is the basis for the substantial disagreement in the relevant literature on the subject.

One of such complications arises when a mixed morphology is present making this situation definitely not suitable to measure time dependence and eventually identify the mechanisms taking place. This is exactly what occurs in processing where a layered morphology is always encountered [43] determined by the superposition of several driving forces during solidification all acting simultaneously: high temperature gradients, high pressures and a melt highly oriented and more or less topologically constrained depending on the stress field applied. Such drastic solidification conditions give rise to a significant departure of the morphology developed from equilibrium [44], which changes through the thickness even determined by different mechanisms of solidification [45].

Unfortunately, many reports on ageing of semicrystalline polymers do not consider such limitations [7–11].

Thus, the CCT approach may help to simplify the interpretation starting with an homogeneous sample that closely mimics processing conditions although only one driving force to solidification, i.e. temperature and its rate of change, is taken in consideration. Unfortunately, such simplification may still leave many complications arising from the size distribution of crystallites due to the non-isothermal history thus making identification of the ageing mechanisms and the separation of the different regimes questionable.

However, this is not all, a severe experimental limitation on studying ageing in crystalline polymers is its sluggishness so that the rate is definitely too small to be measured by any method under laboratory time scale. Although, mechanical properties are sensitive probes often used for the characterization of ageing of polymer glasses, in this case a stress applied can significantly modify the regime where ageing occurs activating, for example, crystalline mobility, even at temperatures lower than quiescent Tαc [46,47] or giving rise to crystallization, if the initial status is mainly amorphous, even below the T_g [48]. Neither an increase of temperature can be used to accelerate ageing presuming the mechanisms do not change. Furthermore, positions of relevant transitions: Tβ, T*, Tαc are still under debate and ageing is used for their measurement [2,31].

Ageing on *i*PP solidified by CCT has been recently studied by simultaneous WAXD and small angle X-ray scattering (SAXS) in the range of 40–80 °C, temperatures typical of sample ejection from a mould in injection molding, with a synchrotron source [32]. Even with the high photon flux available experimental evidence of transformations was observed only for samples mostly mesomorphic for which T* is low. Upon increasing slightly the amount of the α-monoclinic phase a significant decrease in the ageing rate was observed. Changes detected in the WAXD and SAXS patterns are on the limit of instrumental sensitivity, i.e. differences between patterns might be comparable to the error arising from quantitative determinations. In spite of such limits, the significant decrease in the ageing rate with increasing α-monoclinic phase content, probably related to the increase of T* [31], fully accounts for the influence initial morphology has on ageing rate.

Alternative experimental probes must be found if lower temperatures or lower cooling rates initial conditions are to be analyzed. Density might be used when differences between the values of component phases are large enough as it is the case for *i*PP [49]. As a result realtime density measurements have already been made by density gradient column [50] to describe what was interpreted as an overall phenomenon of secondary crystallization in *i*PP. To our knowledge, this is probably the only attempt made on using the time dependence of a sample falling in a density gradient column to describe the density evolution in polymer samples and it has not seen any follow up probably due to the difficulties the method poses.

In this work, the rationale of density measurement in real time by density gradient column is described skipping all the details related to samples preparation, already fully described elsewhere [26]. This approach, although initiated a few years ago, was faced with unpredictable obstacles, which are the subject of this paper. Accounting of all of them gave us the possibility to describe with reproducibility the density evolution of an *i*PP at moderate temperatures. Materials used are listed in Table 1, together with their molecular characteristics, and the solidification curves, i.e. the density dependence on cooling rate for all of them, are shown in Figs. 2 and 3.

4. Density as a morphological probe for ageing in *i*PP

In amorphous polymers, a density increase is always observed upon ageing and it takes place in parallel with a decrease of other state variables, although often with a different time dependence [1,3]. In the case of crystalline polymers changes in mechanical properties may point out remarkable ageing phenomena not necessarily accompanied by relevant changes in density [51]. In this case the three transition temperatures Tβ, T*, Tαc, conventionally related to the three component phases: amorphous, mesomorphic and crystalline, determine the regime where ageing occurs. For crystalline PET, for which Tαc is close to melting, the two mechanisms responsible for ageing should be associated, at low temperature, only to Tβ and T* without significant changes in density. This interpretation is in line with the assumption that the density of the so called mesomorphic phase in PET is close to that of the amorphous phase [42]. Different is the situation for *i*PP where, also at low temperature, if ageing occurs below Tαc, although Tβ, and T* may be the only active mechanisms, the density 'contrast' between amorphous and mesomorphic phases may be sufficient to be detected [49] by density measurements.

Density gradient column is an effective and fast method for measuring density with high accuracy. Much of the unreliability on the results obtained depends on the column preparation, which we suppose to be such that the gradient is constant and therefore, skip all the experimental details, which are covered even in reports of standard methods [52]. Absolute density values depend on the precision of calibration floats. Moreover, accuracy on the density difference does not have in principle an upper bound since a column may be used as a calibration standard, giving thus the possibility to discretize indefinitely the starting density interval. However, with this principle one may end up measuring density differences with only an approximate knowledge of the density neighbor and relative density measurements may be far more accurate than the absolute ones.

With this tool one attempts to overcome the limitations of SAXS/WAXD in the characterization of aged samples [32] and extend the quantitative evaluation of morphology evolution also to low cooling rate samples in which the mesomorphic phase is not prevailing and hence a slower ageing rate is expected. Alternatively it may also be attempted to explore the possibility of applying such methodology to fully mesomorphic samples as well where changes observed in the SAXS

invariant over time are very small for low temperatures, i.e. close to room temperature, more plausible for ageing.

During density determination in a gradient column, a significant limitation arises if density keeps on increasing with time, i.e. the sample does not attain a stable position, thus a recognizable density. Even assuming that the sample is in equilibrium, a continuous change of position can occur if the sample absorbs the solvent/s in which it is immersed. In this case the sample does not sink to its equilibrium density but to that determined by solvent swelling. An equilibrium density value can still be obtained by an extrapolation procedure as adopted for polyamides [26,53] using a fluid dynamics model of a body falling in a viscous medium having a constant density gradient, $G = \mathrm{d}\rho/\mathrm{d}h$:

$$\frac{d\mathrm{h}}{d\mathrm{t}} = \frac{W}{K}\left[\left(1-\frac{\rho_\mathrm{k}}{\rho_\infty}\right) - G\frac{h}{\rho_\infty}\right] \quad (1)$$

where $\mathrm{d}h/\mathrm{d}t$ is the downward velocity, W is sample weight, K is the ratio between the drag force and velocity, ρ_∞ is sample density, and h is the depth from a level where liquid density is ρ_k.

Obviously, the density change at long times can reveal other densification mechanisms occurring in the sample, which may be related, other than to sorption also to morphological ageing. If the time scale in which sorption/ageing takes place is not comparable to that required for the sample to reach its equilibrium position, identification of other densification mechanisms is easy. Eq. (1) can help to separate fluid dynamic transient, it provides a linear relationship between the downward velocity $\mathrm{d}h/\mathrm{d}t$ and the position h, since G is a constant mapping density to the vertical coordinate. Short time falling down behavior is expected to be represented by a straight line in the $\mathrm{d}h/\mathrm{d}t$ vs h plane, if sorption/ageing is negligible. As the value of h at the equilibrium point (h_∞) can be obtained form Eq. (1) for $\mathrm{d}h/\mathrm{d}t = 0$, a linear extrapolation of the data at zero velocity leads to the 'equilibrium density' determination, i.e. of ρ_∞.

Data shown in Figs. 2 and 3, the solidification curves, are based on measurements at low temperature, around 2–3 °C, and all density measurements are then compared at 20 °C using a constant expansion coefficient of 1.5×10^{-4} °C-1 [54]. This way densification due to morphological ageing becomes negligible and accurate values are obtained since there is no measurable interaction between *i*PP and the water–ethanol solution system used for the gradient column. The error due to neglecting the different expansion coefficients of the component phases and their respective amounts is definitely smaller than the one associated with the estimation of the amount of the component phases themselves for which a rationale is not known except for the case where a significant amount of mesomorphic phase is present [49]. Moreover, the error is limited also by the small density changes taking place.

Density after ageing at temperatures of 20, 40, 60 and 80 °C was measured on *i*PP1 samples solidified at cooling rates of 2, 10, 100 and 1000 °C/s and on *i*PP3 samples solidified at 100 and 1000 °C/s. Density was measured offline at 2–3 °C after ageing for times ranging from 30 to 10,000 min. The ageing time intervals were chosen on a half-decade basis in a logarithmic scale. After each such ageing time, the samples were removed from the constant temperature bath used for the ageing and immediately quenched in ice water. Since, for every condition (ageing time and temperature and thermal history) at least three density measurements were necessary to reduce error propagation, the number of samples produced by the CCT procedure and subsequently tested was very high.

The results, reported in terms of percent density increase with time in Fig. 5(a) and (b), for *i*PP1 and *i*PP3, respectively, show an apparently confused scenario. This is because the two parameters (cooling rate and ageing temperature) in the figures, have increased the number of data sets shown. It is, however, useful to compare the trends observed with such parameters since one would also visually compare a dependence on initial morphology out of the expected logarithmic trend as usually reported for a 'secondary crystallization' mechanism [36,50,55]. A closer inspection shows that some data sets do indeed follow such a trend although with a significant scatter due to error propagation resulting from the different techniques used all the way from the sample preparation to density measurement. It is to be recalled that each data point is the result of a sample solidified at the reported nominal cooling rate, which is then held for the specified ageing time at the reported temperature and whose density is measured in a

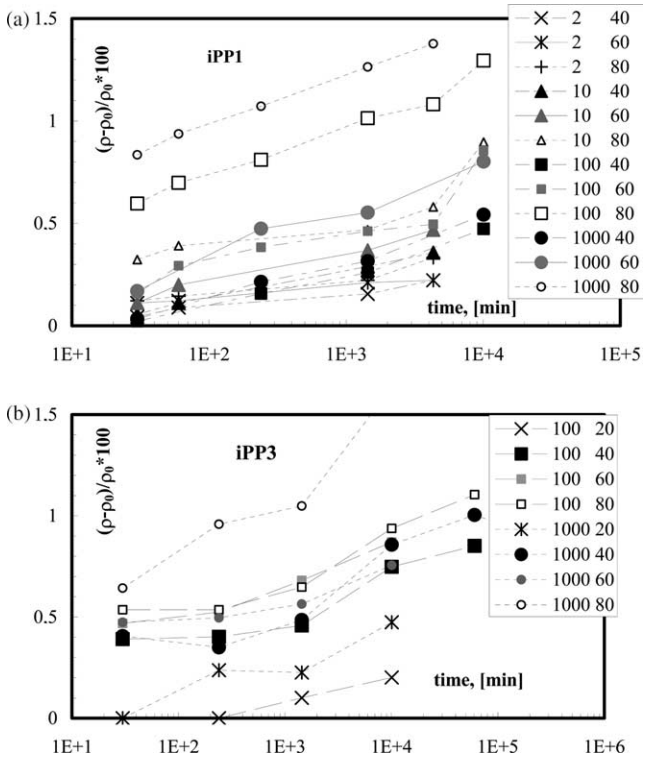

Fig. 5. Relative density increment, in %, vs time for samples solidified at different cooling rates (on the left in the legend) and aged at several temperatures (on the right in the legend). Densities were measured under the same conditions after ageing. ρ_0 is initial density before ageing. (a) and (b) show data referred to *i*PP1 and *i*PP3, respectively.

gradient column. Although, it is difficult to make an estimate of the overall error, which would require an enormously high number of samples to be accurate, a lower bound may be in the range of 15–20% of the final density measured, the worst being referred to lower temperatures. Certainly, in view of such an error, comparison of the data may be questionable. Nevertheless, a trend can be identified thus providing sufficient information, as no other evidence is available. To help reveal such a trend data points are joined as a guide for the eye.

Fig. 5(a) and (b) confirm that higher cooling rate samples show a higher density increase other than, obviously, for increasing temperatures. The density change/increase during ageing at 80 °C is definitely more pronounced for mesomorphic samples, i.e. for cooling rates of 100 and 1000 °C/s in the case of *i*PP1 and 1000 °C/s for *i*PP3. The solidification curves in Fig. 3 point out that the *i*PP3 sample cooled at 100 °C/s is not as completely mesomorphic as the previous ones since it is just at the Q_{cr} for *i*PP3. The small amount of the stable α-monoclinic phase observed in such conditions [49] is such that at 80 °C ageing, this sample tends to behave similar to all other conditions and in particular a linear logarithmic trend is not as obvious as it is for the mesomorphic samples. In some circumstances one may even observe a slower density growth eventually followed by a faster one, as the *i*PP3 samples 100 and 1000 °C/s show more apparently than the others during ageing at 40 °C. If this behavior is correct this would be one evidence that a deviation from the linear logarithmic trend is not at all impossible pointing out that the ageing mechanism is more complicated and that the linear logarithmic trend is rather an overall behavior often encountered due to scarce sensitivity of the log function at long times and the superposition of several combined mechanisms eventually providing compensating effects. Although data at lower temperatures and lower cooling rates could apparently agree with the linear logarithmic behavior, the increased scatter and lower sensitivity may question this conclusion.

The overall slopes observed in Fig. 5(a) and (b) on a log time scale are not much different for all samples except for the fully mesomorphic samples aged at 80 °C, i.e. for both *i*PP1 samples solidified at 100 and 1000 °C/s and *i*PP3 at 1000 °C/s. In all other cases, differences in the absolute density increase are not due to the rate of the process, i.e. the slopes, in the time window of the measurement, but rather to the initial values measured at the smallest available time resolved. The apparent increase of the slope at sufficiently long times for smaller temperatures and cooling rates could suggest onset of a similar process but with a much longer characteristic time. In this event the time/structure window available by each of the measurements given in Fig. 5(a) and (b) is but a very limited view of the ageing mechanisms occurring.

The information provided by Fig. 5(a) and (b), with the available level of resolution, which is very poor indeed, indicate that the polymer used, with the presence of nucleating agents of different concentrations (catalytic residues in the case of *i*PP3 as opposed to *i*PP1, Fig. 3), do not make much difference in the suggestions one may draw from these data. Apart from the temperature, the most important factor determining ageing is the morphology, which in the simple situation under scrutiny, i.e. for samples solidified by CCT, this boils down to the cooling rate at which the material is solidified.

5. Apparent time density evolution

The conclusions drawn from Fig. 5(a) and (b) are rather ambitious and are apparently grounded but on a collection of scattered data. Clearly the picture one draws is definitely influenced by the existing literature [12,20,31,34]. Improving the significance of the information is definitely necessary since the approach of measuring density in *i*PP as a result of ageing in connection with samples of different morphologies, produced by CCT, shows the potential to discriminate their different behavior, evident although embryonic in Fig. 5(a) and (b).

A simple way of reducing error propagation can be provided by the possibility to measure density evolution on the same sample at different times following its position in the gradient column. The method would definitely increase reliability of the information since density can be measured relative to its initial position taking into account the fluid dynamic transient, FDT, by Eq. (1) and recalling that a gradient column has an infinite resolution in terms of relative density. Most of the error would thus be related to the method used for sample production, initial morphology being dependent on the procedure adopted for solidification [26].

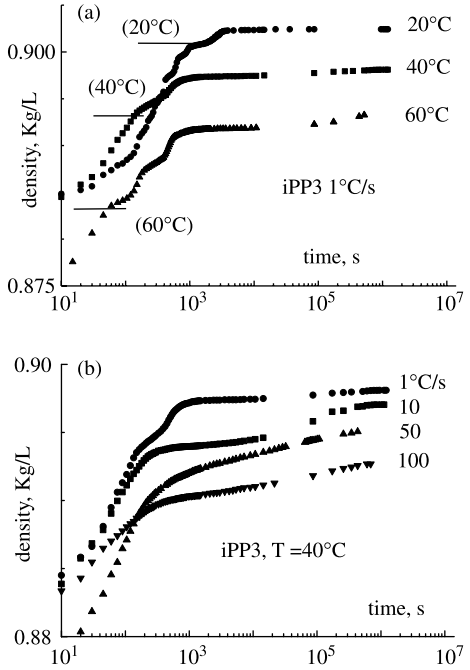

Fig. 6. Apparent density evolution for samples of *i*PP3 falling in a density gradient column with time. (a) Compares the influence of column conditioning temperature on a sample solidified at 1 °C/s. (b) compares the influence of cooling rate on samples solidified at different cooling rates, column is conditioned at 40 °C. In (a) also samples' densities at measurement temperature before ageing, ρ_∞, are estimated from expansion coefficients shown in Table 2.

Fig. 6(a) shows the density dependence on ageing time obtained by recording the path of an average of three samples of *i*PP3 solidified at 1 °C/s and falling in three gradient columns conditioned at three different temperatures. The columns at 20 and 40 °C were filled with a water–ethyl alcohol solution system while the one maintained at 60 °C was filled with an ethylene glycol–butyl alcohol solution system. Similar results are shown in Fig. 6(b) where *i*PP3 samples solidified at cooling rates of 1, 10, 100, 1000 °C/s are compared at a temperature of 40 °C. On the ordinate of Fig. 6(a) and (b) densities are conventionally reported although they are representative of a sample density only after the sample has settled to its equilibrium position as determined by Eq. (1). The previous, only apparent, density excursion depends on the FDT and the regime attained is described by Eq. (1) only if it is laminar and the asset, i.e. the position of the sample during its path, does not change. Since, the sample is often volumetrically irregular (at best a circular disk), often complex flow situations such as tumbling and/or non-laminar regime are observed at short times thus introducing deviations with respect to Eq. (1). Although, it should have been more appropriate to show these results in terms of heights, the difficulty on identifying a common reference height for different columns has necessitated to compare the trends by referring to the apparent densities, obtained by the calibration gradient for each column. Density time dependence, averaged over three samples, is smooth thus significantly improving the observations of Fig. 5(a) and (b).

A common feature of the results shown in Fig. 6(a) and (b) is that density is not constant even at long times, although time dependence is in contrast with previous observations [50,55] since stepwise changes are apparently observed rather than a smooth logarithmic time dependence. The plateaus are characterized by a vanishing slope, i.e. by a negligible rate of density increase and, if multiple plateaus are observed, they are joined by an S shaped density increase in log time, a step for which a characteristic time can be defined as the time at which a maximum rate of density change is observed. The integral of Eq. (1), describing the FDT, yields an exponential time dependence from which also a characteristic time can be drawn, τ_f

$$\tau_f = \frac{K\rho_\infty}{WG} \tag{2}$$

If the structural densification due to morphological ageing takes place with very long times in comparison with τ_f, then one can in principle justify some of the observations shown in Fig. 6(a) and (b). In this case, a plateau density would be attained before the continuous density increase due to morphological ageing. The generality, with multiple steps and plateaus, is however, hard to classify. Some of the results of Fig. 6(a) apparently point out that the influence of temperature is not fully accounted for in the density rate of change but for a delay of a few step-like density increments, clearly shown, making them appear at longer times for lower temperatures.

The question is whether the step-like density increments are due to fluid dynamic perturbations or if they are a result of morphological ageing. Undoubtedly density steps may arise due to perturbations in the 'asset' of the sample on its path. However, a wishful thinking could attribute their onset, i.e. the time at which the slope attains its maximum value, to the characteristic time of transitions occurring in *i*PP. Upon following such an appealing hypothesis, the first flex could be related to a release of mobility of the intermediate phase, i.e. T* and the second to the occurrence of mobility within the crystalline phase by the active Tαc process. Occurrence of Tαc at a temperature lower than the usual value could be justified by its relationship with the crystallization temperature [12], which is lower for a fast solidification process. Temperature dependence of each transition, once unambiguously identified in Fig. 6(a), could even provide an apparent activation energy for each transition thus evidencing its kinetic nature [56]. For this hypothesis to be consistent it is necessary that the apparent density of the solid, i.e. the initial density before any ageing occurs, be smaller than the density at which any plateau occurs.

The initial densities, also shown in Fig. 6(a), were obtained assuming a constant volume expansion coefficient dependent on cooling rate as given in Table 2 [54]. Furthermore, it was assumed that at the column heating rate of 0.033 °C/min used for their estimation, and within the range of temperatures used (between −15 and 10 °C), the samples are stable at their initial density values, ρ_∞, the ones corresponding to the solidification conditions adopted before any ageing takes place. Since, during heating, ageing takes place entailing a density increase, the values reported in Table 2 for the volume expansion coefficient should be taken as lower bounds only.

The correct expansion coefficients, corresponding to the structure associated to the cooling rate used for the solidification, could thus be obtained only upon extrapolating the values of the expansion coefficients obtained upon increasing the heating rates used for their measurement. Such possibility, which would consider negligible morphological ageing when heating rate is a sufficiently faster process, is clearly hard to reach when using a massive gradient column to measure the expansion coefficient through density changes [54]. Thus, one observed that the expansion coefficient measured during heating is greater than that obtained during cooling and final density at the initial temperature used for the

Table 2
Initial densities, expansion coefficients and slope of the logarithmic, with time, density increase, SL, of morphological ageing.

Cooling rate (°C/s)	Ageing temperature (°C)	SL, $\Delta\rho/\Delta\log(t)$ (Kg/L/log(s)$\times 10^{-3}$)	Volume expansion coefficient ($^\circ K^{-1}$)	Predicted initial density (Kg/L)
1	20	0.38	1.5×10^{-4}	0.899
15	20	0.66	1.5×10^{-4}	0.894
100	20	0.62	3.0×10^{-4}	0.884
1	40	0.85		0.896
15	40	1.18		0.892
100	40	1.19		0.877

Influence of cooling rate and temperature.

cycle is higher than the starting one. For low cooling rate samples, 1 °C/s, such an increase is moderate, i.e. ca. 10%, whereas for higher cooling rate samples the expansion coefficients may be severely underestimated [54].

A more complex scenario appears upon comparing the density evolution at a temperature of 40 °C for samples solidified at different cooling rates in Fig. 6(b). For lower cooling rates, 1 and 10 °C/s, a behavior similar to that reported in Fig. 6(a) for the temperature dependence of density evolution for the 1 °C/s sample, is observed. Here again, step-like density increments and density plateaus could be reconciled with the idea of multiple transitions although their occurrence and their order might be difficult to assign to a specific transition. Considering density evolutions of different cooling rate samples at all other temperatures tested does not help either and therefore, are not reported here. The density evolution of higher cooling rate samples without any apparent step-like density increments is even more obscure. The possibility that some transitions are masked by the FDT could be the only alternative explanation to justify the relative position of the step-like density increments observed for different samples since one would expect the same transition to occur at lower times for increasing cooling rates at a given temperature or, alternatively, at lower times for the same cooling rate upon increasing temperature. Unfortunately, a clear scenario is not available although an attempt to reconcile the temperature and cooling rate dependence has been made driven by the enthusiasm of such a broad set of new information [56].

6. Real time density measurements

Clearly for high cooling rate samples densification related to morphological ageing starts while the position in the column is not yet at the initial value, i.e. this densification mechanism is superimposed with the fluid dynamic transient, FDT. Thus, the possibility to follow densification related to morphological ageing at times comparable with τ_f is ruled out by the superposition with the FDT unless Eq. (1) were a reasonable description of the phenomenon.

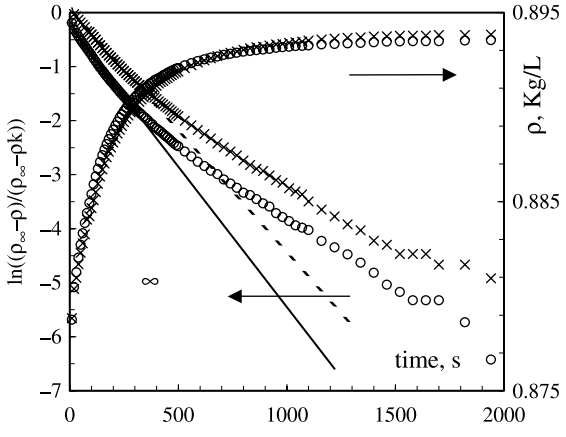

Fig. 7. Apparent density evolution for two stable samples of *i*PP3, i.e. thoroughly aged at measurement temperature, falling in a density gradient column with time. On the left ordinate the logarithm of normalized density is also shown. ρ_∞ is samples' density, constant with time for these samples, and ρ_k is a fitting parameter approximately corresponding to the density where onset of laminar flow is attained, see text. Sample path is free of any obstacle and column is conditioned at 40 °C.

Fig. 7 shows the apparent density evolution of a stable sample, i.e. a sample already aged at the same temperature at which the density is measured for much longer times than the largest recorded. Since, sample density reaches a constant value at long times it is obviously in equilibrium at the measurement temperature. Fig. 7 also shows, on the left ordinate, the normalized density evolutions in a logarithmic scale for the same samples. A tentative fitting with Eq. (1), which is linear in the log vs time plane, is also shown since the data in Fig. 7 are representative only of fluid dynamic contributions. Analyzing the parameters in Eqs. (1) and (2) it can be seen that the characteristic time of the FDT, τ_f, increases with viscosity (through the drag force coefficient, K) and decreases with density gradient, G. Other parameters include the density of the solid and the density at which the fall down starts, i.e. ρ_∞ and ρ_k, respectively. Since, ρ_∞ is fixed, ρ_k might be a fitting parameter dependent on several causes sometimes concurrent: onset of turbulent flow before a laminar regime is attained or influence of non-laminar regime on the asset of the sample, which might oppose a complex transverse area to flow direction. However, changing ρ_k and τ_f is not sufficient to fit the data in Fig. 7. The logarithm of the normalized apparent density increase due to FDT cannot be represented by a linear function even if one excludes from the fitting a significant portion of initial data. Clearly long time apparent density time dependence, due only to the FDT, becomes slower than Eq. (1) would predict.

Results in Fig. 7 clearly show that Eq. (1) is not obeyed when the sample is close to its equilibrium position, i.e. when its velocity is low. Upon estimating the size of the boundary layer around the sample, assuming an equivalent hydraulic radius of the same order as the disk radius (the sample), one observes that it becomes comparable to the size of the column when the sample approaches its equilibrium position. This happens because velocity decreases, as Eq. (1) shows, and the boundary layer diverges with the velocity tending to zero [57]. Occurrence of boundary layer phenomena also explain some of the anomalies encountered in Fig. 6(a) and (b) where step-like density increments are observed after density plateaus, i.e. zones where the velocity decreases. In these zones, the sample slows down since the radius of the column decreases due to the presence of obstacles, i.e. either other samples or calibration floats. Interpolations accounting of boundary layer effects and related phenomena show that the velocity decrease, when traveling in a medium of limited dimensions, depends only on the ratio of the diameters between the particle, assumed spherical, to the column diameter (Francis' correlation [58]). Furthermore, the influence of obstacles can be taken into account by an equivalent hydraulic radius given by the transverse area divided by its perimeter. Assumption shown to be correct, whichever the shape of the obstacle and thus of the cross-section, for vanishing velocities [59]. Although, Francis correlation takes into account that the sample does not

travel in an unbounded medium and therefore, the terminal velocity should be smaller, it does not introduce any correction for the velocity dependence on the driving force to flow when boundary layer effects are significant. Due to its empirical source it supplies only a constant correction to the limiting velocity dependent on the sample to column diameter ratio. Since, the boundary layer increases when the sample is close to its equilibrium position, becoming comparable to the size of the column, one would expect a different regime to take place and the correction for the terminal velocity should account of this change. Eq. (1) and any reported correlation [58] do not take into account of this change of regime and improved analyses must be conceived.

Uncertainties on the interpretation of the data shown in Fig. 6(a) and (b) are now reasonably explained since a change of sample velocity may be negligible if the boundary layer dimension is small, for example, when sample falling velocity is large, or when an obstacle, being crossed by the sample on its path, is farther away from sample equilibrium position. A plateau, however, may be expected if the obstacle is close to sample equilibrium position since Eq. (1) gives in this case a velocity linearly decreasing with distance from equilibrium.

In spite of the difficulty connected to the interpretation of the FDT, the results of Fig. 7, however, show that a significant improvement can be obtained once also sources of errors related to the increase of the boundary layer, when the sample approaches its equilibrium position, are avoided. This is done by following the time history of the sample sinking in a column where any obstacle in its path, including the calibration floats, are avoided. Although, they are necessary to translate sample path into density evolution, they are immersed only after recording the samples' apparent density evolution.

The data of Fig. 8 are obtained with the same procedure although they refer to so called 'fresh samples' solidified at cooling rates of 1, 15 and 100 °C/s of *i*PP4, as reported in Table 1. Two ageing temperatures, 20 and 40 °C, were tested in a column filled with a solution system of water and ethanol. Fig. 8 thus shows the cumulative density evolution due to the apparent density change towards the initial density, related with the FDT, and the density evolution due to the morphological changes taking place upon ageing, as previously defined. All the curves demonstrate the presence of these two phenomena although with different time dependences, the former being faster than the latter. Albeit such evidence, the discussion of the equilibrium samples reported in Fig. 7 clearly points out that a quantitative separation of the two mechanisms appears rather difficult since no clear cut is shown by the data, even those referred to the sample solidified at 1 °C/s aged at 20 °C. As the two mechanisms tend to merge with increasing cooling rate and temperature, the difficulty for their separate interpretation clearly grows.

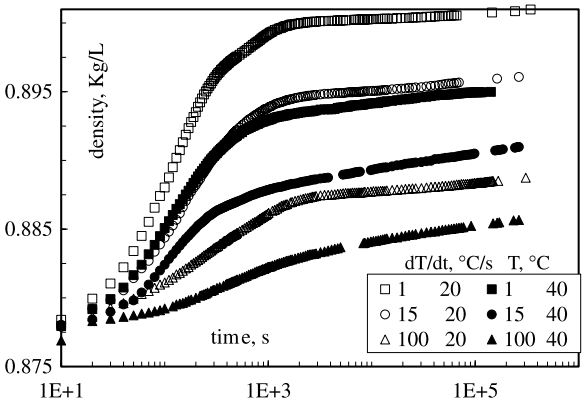

Fig. 8. Influence of cooling rate and column conditioning temperature on apparent density evolution for samples of *i*PP4 falling in a density gradient column with time. Sample path is free of any obstacle.

The low temperature (20 °C) curves show a distinct change of curvature at very similar times except for the 100 °C/s sample, which is shifted to slightly longer times in contrast with the smaller ρ_∞, see Eq. (2). If one could draw a characteristic time for the low temperature data (20 °C) using Eq. (1) for the FDT, the contribution due to the FDT turns out to be clearly distinguishable with respect to that of the ageing behavior. It can also be observed that the portion of the ageing behavior that is not superimposed on the FDT is roughly linear in the log time scale apparently confirming previous observations [50,54].

At the higher temperature, 40 °C, the behavior becomes more complicated and as a result there is no common range of times where a clear distinction of the two mechanisms can be made. For the 100 °C/s sample no clear distinction of the two mechanisms is even possible. It should be expected, however that, if sample weight and column density gradient are approximately constant, the FDT moves towards smaller times at 40 °C since a smaller viscosity implies a reduction of the drag force coefficient, K, in Eq. (2) and consequently of τ_f, implying the possibility to extend the resolution of the densification related to morphological ageing to smaller times. This is apparently the case for the 1 °C/s sample for which an apparent change of densification mechanism moves to smaller times on increasing temperature from 20 to 40 °C. For the 100 °C/s there is, however, a clear shift for the change of curvature to definitely longer times with respect to the lower cooling rate samples and such feature is enhanced at higher temperature.

If one neglects the upward curvature observed at 20 °C for samples solidified at 1 and 15 °C/s, a slope of the logarithmic, with time, density increase can be derived from longer time data, SL. Although, visual inspection does not show much changes of SL between samples solidified at different thermal histories, a systematic trend for SL can be observed from the values shown in Table 2, for which an average error of ca. 7% has been estimated on comparing several samples solidified at similar cooling rates. Table 2 confirms that a significant change of SL, of ca. 100%, takes place upon increasing temperature from 20 to 40 °C. Differences related to thermal history, i.e. to initial morphology, are however, mostly observed between the low cooling rate sample, 1 °C/s, and the rest; therefore increments of SL of ca. 60 and 35% are observed at 20 °C and at 40 °C, respectively, upon increasing cooling rate to 15 or 100 °C/s. Differences of SL between the latter samples are negligible although these are comprised in a quite broad

interval of initial morphologies, ranging from a sample of roughly 38% α-monoclinic phase content [60] up to a completely mesomorphic one with but unmeasurable traces of α-monoclinic phase. It is then clear that the differences in the FDT must bear the missing information since, for a larger cooling rate sample one expects a larger departure from equilibrium and thus a more pronounced ageing, whichever it will be its evidence, either a larger rate or a larger density increase and sometimes both.

A density jump at small times would be justified if the density change accounted by the logarithmic increase is smaller than the overall expected to take place based on the initial sample density at the same temperature. Unfortunately, the poor resolution before the linear log density increase and the limitations on the interpretation of the FDT jeopardize the possibility to accurately measure the initial density of the sample. If the lower bounds for the expansion coefficients reported in Table 2 are used, the density values, also reported in Table 2, would be obtained on the basis of the solidification curve for *i*PP4 reported in Fig. 3. Comparison of these data with the results shown in Fig. 8 makes clear that the initial densities of samples solidified at 1 and 15 °C/s at 40 °C are clearly overestimated. This depends on the parallel underestimate of the expansion coefficient, as previously explained, since it is measured on a sample, which ages, i.e. density increases while it is being measured. Such underestimate is reasonably expected to be even more pronounced for the 100 °C/s sample.

Upon extrapolating the linear log increase, for the 100 °C/s sample, to a time of 1 s one finds a density larger than the one reported in Table 2, derived from the expansion coefficient and clearly overestimated. For the 1 and 15 °C/s samples one observes the opposite trend: although the densities obtained by the expansion coefficients are overestimated, the density value extrapolated from SL to 1 s is smaller than the densities reported in Table 2. One may conclude that a significant increase of density must take place at short times for the 100 °C/s sample, however, not detectable since mostly superimposed with the FDT. Thus, although no significant differences in the SL are observed between the 15 and 100 °C/s samples, their plausible different morphological ageing behavior should be related to a fast density jump, which is, however, very difficult to detect and to translate into quantitative information. If this hypothesis is correct, the mesomorphic sample should be characterized by onset of mobility at a temperature significantly lower than the one of α-monoclinic crystalline samples. The same conclusion could have also been drawn from the data in Fig. 5(a) and (b) had they been less scattered. A posteriori one can interpret the apparent density increase shown by the mesomorphic samples of *i*PP1 cooled at 100 and 1000 °C/s and that of *i*PP3 cooled at 1000 °C/s, at smaller times compared with the data at longer times.

If this observation is correct then one sorts out with a dichotomy: on one side low cooling rate samples, where ageing has been supposed to depend on cooling rate by a change of SL alone, and on the other side the mesomorphic ones, where an abrupt change of density takes place at times much smaller to be measurable with the available time resolution, eventually followed by a lower rate of density change with the logarithm of the time. The doubt arises on observing Fig. 2 where the range of cooling rates where coexistence of α-monoclinic and mesomorphic phases is broad, particularly for the *i*PP4 the data shown in Fig. 8 refer to. One may wonder whether such a dichotomy rather depends on the ignorance of the true initial density, or that is the same, of the true expansion coefficient. The subject definitely deserves further investigation starting with an improved estimate of the true expansion coefficient and its dependence on initial morphology. A better description of the FDT is, however, also necessary since it would permit to increase the resolution in the lower time region of the phenomenon where not much experimental advances can be made. Although, a faster FDT would be available increasing the gradient, *G*, or decreasing solvents viscosity, the first method would decrease resolution and the second cannot be pursued to any relevant extent with common solvents.

Many are therefore the open questions, all of which having certain technological relevance, concerning the significance of the density jump before the linear density increase seen in the semi-logarithmic plot of the density against time, whether it is activated above a certain threshold temperature or below a threshold amount of the stable crystalline phase, which would otherwise act as cross-links. Moreover, this density–time relationship should be expected to depend in a complex way on temperature and initial morphology. Elucidating all these features would probably permit to reconcile the experimental behavior with the idea that the onset of mobility on different domains determines morphological ageing.

7. Conclusions

Ageing in crystalline polymers depends on the mutual transformation of stable and metastable phases. So, hereafter, it is referred to as 'Morphological ageing' as it is always related to changes in morphological organization. It is mechanistically different with respect to physical ageing, usually referred to metastable glasses, since in crystalline polymers the multiple phase composition with amorphous phases of different mobility and eventually multiple crystalline phases significantly complicate the scenario. In the simplest situation, one could assume three main mechanisms to determine the ageing regime: the beta relaxation associated with onset of mobility of the amorphous phase, Tβ, a similar mechanism taking place at larger temperature to be ascribed to the constrained, by the crystalline domains, disordered phase, T*, and finally by onset of mobility in the crystalline phase, Tαc. The latter being effective when a low temperature such mechanism exists since only in this case it is relevant to ageing [35,36]. Despite this complex scenario available information always shows a linear logarithmic time dependence of the relevant morphology or properties dependent parameter investigated.

In this work, a CCT approach is used to study ageing in *i*PP. This method gives the possibility to produce samples of finite dimensions, i.e. macroscopic, designing the morphology on the basis of the cooling rate adopted for their solidification from

the melt. This way one avoids the usual mistake of using non-homogeneous samples thus precluding the possibility to investigate dependence on initial morphology. Furthermore, the cooling rate range matches the typical conditions met in processing where high thermal gradients are usually encountered. Albeit the drastic cooling, homogeneity is preserved even at the highest cooling rates adopted giving the possibility to approach the ageing behavior of samples in which the departure from equilibrium is rather pronounced.

Previous studies using SAXS and WAXD as structural probes confirmed the linear log dependence on time although the low sensitivity has limited the application to mostly mesomorphic samples. Mechanical properties, although sensitive probes, are a complex effect of morphological ageing so that their relationship with the underlying mechanisms are difficult to interpret. Alternatives must therefore be identified if one wants to extend the investigation to low cooling rates or low temperatures, that are more usual to ageing.

Since density contrast among the three phases, schematically identified in *i*PP: amorphous, mesomorphic and α-monoclinic, should be sufficient [49] to account of possible transformations among them, density was used as a morphological probe. It was measured by the gradient column technique with two methods: ageing off line the sample and measuring the density always under the same conditions, and online following sample density evolution with time in the column conditioned at the ageing temperature.

The first method gives quite a broad scatter since each measurement is the result of a cumulative addition of possible errors arising from sample preparation, ageing and from individual density measurements possibly made in different columns. However, it is possible to identify the remarkable role of temperature on ageing and the different behavior arising as a consequence of different initial morphology, i.e. cooling rate. The dependence is clear for high cooling rate samples and less pronounced for the lower cooling rate samples due to the scatter of the results. Comparison of two different *i*PP's confirms previous SAXS results in that morphology determines the different response to ageing rather than the polymer with its molecular characteristics.

With the second method density cannot be measured directly since it is coupled with the fluid dynamic transient, FDT, related to the sample sinking towards its equilibrium density in case it does not age. Measurements of apparent density dependence on time on non-equilibrium samples characterized by different initial morphologies, i.e. cooling rates, at temperatures of 20, 40 and 60 °C, showed a peculiar behavior with step-like increments of density. Finally, one would aim to relate them with the expected thermal transitions if they are determined by different characteristic times. Unfortunately, contradictions in the characteristic time dependence on initial morphology and a study of the FDT reveal the weakness of such measurements that are prone to the influence of geometrical obstacles present along the path the sample describes towards its equilibrium position.

Perturbations arise because, upon approaching equilibrium, velocity decreases and the size of the boundary layer around the sample, which is inversely proportional to it, becomes comparable to the column size such that every obstacle along the path slows down the sample. Accounting of such a restriction, step-like transitions are eliminated and the apparent time density evolution clearly shows two phenomena. At long times density depends on morphological ageing and at short times on FDT. Their separate interpretation is, however, possible only at low temperatures for low cooling rate samples since in this case one observes even a density plateau before the densification related to morphological ageing takes place. At higher cooling rates and higher temperatures separation would require a thorough description of the FDT, not yet possible from available correlations.

At times sufficiently larger than the characteristic one for the FDT, density evolution shows the typical linear increase with the logarithm of time. The slope of such a linear trend depends on cooling rate increasing with it, i.e. the slope quantitatively accounts of the initial morphology. However, for higher cooling rate samples, where the mesomorphic phase is prevailing on the stable α-monoclinic one, the slope alone does not account of the different morphology. In this case, an abrupt change of density must take place, which is, however, difficult to detect and to translate into quantitative information as it should have taken place at small times and it is therefore, superimposed on the FDT. If this hypothesis is correct, mesomorphic samples should be characterized by the onset of mobility at a temperature significantly lower than that of the α-monoclinic crystalline samples.

Standing the broad range where the coexistence of the α-monoclinic and the mesomorphic phases are observed in Figs. 2 and 3, one may wonder whether such a dichotomy should be applied or it merely depends on the ignorance about the true initial density and/or the true expansion coefficient. Many are the open questions, all of technological relevance as well. They are concerned with the relative importance of the density jump with respect to the linear logarithmic with time density increase. Whether the density jump is activated above a certain threshold temperature or threshold amount of the stable crystalline phase, which would otherwise act as cross-links. Whether the linear logarithmic with time density increase should be expected to depend on the relevance of the initial density jump, i.e. if the two phenomena mutually influence each other. Elucidating all these features would probably permit to reconcile the experimental behavior with the idea that the onset of mobility on different domains determines morphological ageing.

Acknowledgements

This work is a spin off of a BRITE project that started in 1999. I am most grateful to several students who contributed to this work, started as an undergraduate thesis in 1994. Among them, David Sequeira started the time resolved density measurements during his Erasmus mobility in 1999. David Catalini (Universidad Nacional de Mar del Plata, Argentina) contributed to the final results as part of a Masters degree

within a UE-LA Alpha project (PLastinet). I am grateful to Dr Momchil Botev for enlightening discussions on the interpretation of mobility in crystalline polymers and to Prof. Valerio Brucato for invaluable assistance on the fluid dynamics issues. Finally, many thanks are due to Zebene Kiflie and Enzo La Carruba for reading and commenting the manuscript.

References

[1] Hutchinson JM. Prog Polym Sci 1995;20:703.
[2] Struik LCE. Physical ageing in amorphous polymers and other materials. Amsterdam: Elsevier; 1978.
[3] McKenna G. In: Booth C, Price C, editors. Comprehensive polymer science. Polymer properties, vol. 2. New York: Pergamon; 1989. p. 311.
[4] Struik LCE. Polymer 1987;28:1521. Struik LCE. Polymer 1987;28:1534.
[5] Chai CK, McCrum NG. Polymer 1980;21:706.
[6] McCrum N. Polymer 1984;25:299.
[7] Tomlins PE. Polymer 1996;37:3907.
[8] Tomlins PE, Read BE. Polymer 1998;39:355.
[9] Uzomah TC, Ugbolue SCO. J Appl Polym Sci 1997;65:625.
[10] Ibhadon AO. J Appl Polym Sci 1996;62:1843.
[11] Hellinckx S. Colloid Polym Sci 1997;275:116.
[12] Rault J. J Macromol Sci, Rev Macromol Chem Phys 1997;C37:335.
[13] Fiebig J, Gahleitner M, Paulik C, Wolfschwenger J. Polym Testing 2002; 18:257.
[14] Wang TH, Young WB, Wang J. Int Polym Process 2002;17:146.
[15] Boudou L, Guastavino J. J Phys D: Appl Phys 2002;35:1.
[16] Kumar B, Koka S, Rodrigues SJ, Nookala M. Solid State Ion 2003;156: 163.
[17] Ayad R, Safa L, Bureau G, Marull S. J Test Eval 2002;30:55.
[18] Liao SJ, Chang DY, Chen HJ, Tsou LS, Ho JR, Yau HT, et al. Polym Eng Sci 2004;44:917.
[19] Michaeli W, Starke C. J Polym Eng 2004;24:289.
[20] Rault J. Crystallization process of polymers: adsorption and annealing. In: Dosiere M, editor. Crystallization of polymers. Dordrecht: Kluwer Academic Publishers; 1993. p. 313.
[21] Strobl G. Eur Phys J 2000;E3:165.
[22] Wunderlich B. Macromolecular physics. Crystal melting, vol. 3. London: Academic Press; 1980.
[23] Bershtein VA, Egorov VM. Differential scanning calorimetry of polymers. Chichester, UK: Hellis Horwood Ltd; 1994.
[24] Strobl G. Polymer physics. Berlin: Springer; 1999 p. 143.
[25] Ciofalo M, Di Piazza I, Brucato V. Int J Heat Mass Transfer 1999;42: 1157.
[26] Brucato V, Piccarolo S, La Carrubba V. Chem Eng Sci 2002;57:4129.
[27] Piccarolo S. J Macromol Sci, Phys 1992;B31:501.
[28] La Carrubba V, Brucato V, Piccarolo S. Macromol Symp 2002;180:43.
[29] Boyer RF. J Macromol Sci-Phys 1973;B8:503.
[30] Gupta VB. J Appl Polym Sci 2002;83:586.
[31] Botev M., Rault J., Secondary transitions in isotactic polypropylene, paper in preparation.
[32] Martorana A, Piccarolo S, Sapoundjieva D. Macromol Chem Phys 1999; 200:531.
[33] Boyd RH. Polymer 1985;26:323.
[34] Botev M., PhD Thesis Mobilité macromoleculaire et transitions survitreuses dans le polypropylene isotactic, Université de Paris-Sud, 1999.
[35] Hu C, Schmidt-Rohr K. Acta Polymerica 1999;50:271.
[36] VanderHart DL, Snyder CR. Macromolecules 2003;36:4813.
[37] Alizadeh A, Richardson L, Xu J, McCartney S, Marand H, Cheung YW, et al. Macromolecules 1999;32:6221.
[38] Heck B, Hugel T, Iijima M, Sadiku E, Strobl G. New J Phys 1999;1:17.
[39] Kopp S, Wittmann JC, Lotz B. J Mater Sci 1994;29:6159.
[40] Keller A, Cheng SZD. Polymer 1998;39:4461.
[41] Strobl G. Polymer physics. Berlin: Springer; 1999 p. 181.
[42] Wang Z-G, Hsiao BS, Sauer BB, Kampert WG. Polymer 1999;40:4615.
[43] Saiu M, Brucato V, Piccarolo S, Titomanlio G. Int Polym Process 1992;7: 267.
[44] Wang TH, Young WB, Wang J. Int Polym Process 2002;17:146.
[45] Strobl G. polymer physics. Berlin: Springer; 1999 p. 173.
[46] Asada T, Sasada J, Onogi S. Polym J 1972;3:350.
[47] DeCandia F, Iannelli P, Staulo G, Vittoria V. Colloid Polym Sci 1988; 266:608.
[48] Saraf RF, Porter RS. Polym Eng Sci 1988;28:842.
[49] Martorana A, Piccarolo S, Scichilone F. Macromol Chem Phys 1997;198: 597.
[50] Baum J, Schultz JM. J Appl Polym Sci 1981;26:1579.
[51] Kiflie Z, Piccarolo S, Vassileva E. Macromol Symp 2002;185:35.
[52] ASTM D1505-03, Standard test method for density of plastics by the density-gradient technique.
[53] Brucato V, Piccarolo S, Titomanlio G. Int J Forming Processes 1998;1:35.
[54] Botev M, Piccarolo S., Estimate of *i*PP thermal expansion coefficient by gradient column technique, paper in preparation.
[55] Piccarolo S, Sapoundjieva D, Brucato V. Post processing behaviour of semi-crystaline polymers. In: Cunha AM, Fakirov S, editors. Structure development in processing for property enhancement. Nato science series, vol. 370. Dordrecht: Kluwer Academic Publishers; 2000. p. 235.
[56] Piccarolo S., Can quenching experiments answer open questions on non isothermal crystallization? COST P1 on polymer crystallization, Vught NL 16–18 Dec 2000.
[57] Bird RB, Stewart WE, Lightfoot EN.. 2nd ed Transport phenomena. New York: Wiley; 2002 p. 133.
[58] Chhabra RP. Steady non-Newtonian flow about a rigid sphere, Encyclopedia of fluid mechanics. In: Cheremisinoff NP, editor. Flow phenomena and measurement, vol. 1, 1998. p. 983.
[59] Alfano V. Una Metodologia per la Determinazione dell'Evoluzione della Densità in Polimeri Solidificati da Fuso Mediante Colonna a Gradiente, Laurea Thesis, Univ. di Palermo, Nov 2004.
[60] La Carrubba V, Brucato V, Piccarolo S. J Polym Sci, Polym Phys 2002; 40:153.